PAPER

Check for updates

Synergetic effects of bimetals in modified beta zeolite for lactic acid synthesis from biomass-derived carbohydrates†

Meng Xia,[a] Wenjie Dong,[b] Minyan Gu,[a] Cheng Chang,[a] Zheng Shen*[ac] and Yalei Zhang [iD] *[a]

An experimental study was carried out to convert carbohydrates using bimetal modified beta zeolite to obtain a maximum yield of lactic acid. The relationship between the properties and the catalytic performance of various bimetal modified beta zeolites was evaluated. The results showed that the maximum yield of lactic acid reached 52% with more than 99% glucose conversion over Pb–Sn-beta (0.3 mmol g^{-1}, Pb/Sn = 4 : 7) at 190 °C for 2 h under ambient air pressure. To evaluate the synergetic mechanism of lead and tin, key intermediates such as fructose, dihydroxyacetone, glyceraldehyde and pyruvaldehyde were used as probe reactants that were catalyzed by Pb-beta, Sn-beta and Pb–Sn-beta. The revealed key role of lead was to promote the isomerization of glucose to fructose and the retro-aldol condensation reaction from fructose to dihydroxyacetone and glyceraldehyde; meanwhile, tin had a superior catalytic performance in the dehydration of dihydroxyacetone, the hydration of pyruvaldehyde and the isomerization of pyruvic aldehyde hydrate.

1. Introduction

Biomass is sustainable, nontoxic, cheap and abundant in nature. Based on these properties, the efficient utilization of biomass to produce liquid fuels and chemicals has attracted significant attention on a global scale.[1–3] Among the various synthetic chemicals, lactic acid is one of the top 12 bio-based "platform molecules", as a starting point for catalytic synthesis, which can be further catalytically converted into high-value-added chemicals.[4–7] Moreover, lactic acid is also considered a renewable chemical building block for polylactic acid (PLA), which has the potential to replace fossil-derived plastics and to emerge expansive promise in markets.[8] Due to its extensive applications in pharmaceuticals, food industry, cosmetics and biodegradable plastic, the demand for lactic acid has increased.[9] Currently, production of lactic acid mainly includes microbial fermentation, enzymatic and hydrolysis of lactonitrile. Among of these, approximately 70% of lactic acid is harvested by microbial fermentation of carbohydrates in the world,[10–13] although very selective, these biological processes

have several drawbacks related to complex purification, unexpected salt waste effluent and slow kinetics.[14,15] The method of enzymatic and lactonitrile hydrolysis also confront with the high cost of enzyme and using highly toxic hydrogen cyanide, respectively. Based on these problems, alternative chemo-catalytic processes to generate lactic acid or the corresponding esters have been the subject of extensive attention.

In the chemocatalytic process, Hayashi and Sasaki first reported that trioses were catalytically converted into alkyl lactates in alcoholic media by homogenous catalysts in 2005.[16] Since then, other starting materials such as glucose,[17–19] glycerol[20,21] and cellulose[22–24] as well as raw biomass[25,26] also have been explored to generate high yield of lactic acid or its esters in homogenous catalytic system. Among these, Zn, Ni and activated carbon have been found to greatly promote yields of lactic acid from cellulose under alkaline hydrothermal conditions.[27] More significant yields of lactic acid have obtained approximately 70% from conversion of milled cellulose in 20 ml of Pb^{II}NO$_3$ (7 mM); at the same time, theoretical and experimental studies have suggested that lead(II) played a key role in a series of cascading reactions for lactic acid formation.[28] Subsequently, the two-component In–Sn homogenous catalyst system has been demonstrated to effectively synergistically catalyze several elemental reactions for MeLac syntheses from hexoses.[29] These metal species, as homogenous catalysts, have advantages in producing lactic acid or its esters from different materials, but difficulties with separation and recovery from the reaction mixtures. Heterogeneous catalysts can effectively overcome those disadvantages, and they have been extensively researched

[a]State Key Laboratory of Pollution Control and Resources Reuse, Key Laboratory of Yangtze River Water Environment of Ministry of Education, College of Environmental Science and Engineering, Tongji University, Shanghai 200092, China. E-mail: zhangyalei@tongji.edu.cn; shenzheng@tongji.edu.cn

[b]Zhejiang Scientific Research Institute of Transport, Hangzhou 311305, China

[c]National Engineering Research Center of Protected Agriculture, Tongji University, Shanghai 200092, China

† Electronic supplementary information (ESI) available. See DOI: 10.1039/c7ra12533j

in recent years.[30–38] In particular, the Sn-beta zeolite has been applied to obtain 64% methyl lactate directly from sucrose in methanol at 160 °C.[39] However, the yield of lactic acid in aqueous solution was far lower than in an organic solution under the same conditions. Hence, exploring an appropriate catalyst to promote the yield of lactic acid in aqueous solution remains a challenge. The conversion of sugars into lactic acid proceeds *via* a series of complex cascading steps, and different metal species possibly improve different key steps in the catalytic reaction. Based on previous research by our group,[40] we proposed a design strategy that different metal species incorporated into Sn-beta zeolites to further promote the yield and selectivity of lactic acid from carbohydrates conversion in aqueous media.

In the present work, we prepared all kinds of bimetal modified beta zeolite catalysts including different metal loading Pb–Sn-beta as well as Ni, Cu and Ce modified Sn-beta zeolites by solid-state ion-exchange method to convert sugars into lactic acid in aqueous solution under mild conditions. The relationship between the catalytic activity and physicochemical properties of catalysts with different loading of lead and tin in beta zeolites was examined. The effect of reaction conditions on lactic acid yield was evaluated. Moreover, key intermediates such as fructose, dihydroxyacetone, glyceraldehyde and pyruvaldehyde were used as probe reactants that were catalyzed by Pb-beta, Sn-beta and Pb–Sn-beta to discuss the synergistic mechanism of lead and tin, while the reaction route was being proposed.

2. Materials and methods

2.1 Materials

D-(+)-Glucose (99.5%), D-(−)-fructose (99%) and tin(II) acetate were obtained from Sigma-Aldrich. D-(+)-Mannose (99%), lactose (98%), starch, formic acid (≥98%), acetic acid (99.8%), glycolic acid (98%), levulinic acid (99%), oxalic acid (99%), pyruvaldehyde (40%), 1,3-dihydroxyacetone dimer (97%), stannic oxide (99.5%), nickel(II) acetate (99%) and cerium(III) acetate (99%) were purchased from Aladdin. Sucrose (99%), lead (II/IV) oxide (95%), lead(II) acetate (99.5%) and copper(II) acetate (99%) were obtained from the Sinopharm Chemical Reagent Co. Ltd. (Shanghai, China). Cellulose (microcrystalline) and lactic acid (1.0 M) were purchased from Alfa Aesar. 5-Hydroxymethylfurfural (98%) was purchased from J&K Scientific. A commercial beta zeolite (Si/Al ratio of 25) was purchased from Catalyst Plant of Nankai University (Tianjin, China). All reagents were used as-received without further purification.

2.2 Catalyst preparation

The catalysts were prepared by a solid-state ion-exchange following the published protocol.[40,41] The typical procedure was that the beta zeolite (13 g) was treated with an HNO_3 solution (65 wt%, 250 ml) at 100 °C for 20 h, followed by centrifuged and repeatedly washed with deionized water until the supernatant was neutral (pH = 7) to obtain the dealuminated beta zeolite (deAl-beta). Then, the obtained deAl-beta zeolite was dried at 150 °C overnight.

The bimetallic beta zeolites were prepared by grinding deAl-beta (1 g) with the corresponding acetates for 30 min. Subsequently, the samples were calcined in an air flow at 550 °C with a ramp of 2 °C per minute for 360 min. The different lead and tin loading beta zeolites (0.2 mmol g^{-1}, 0.4 mmol g^{-1}, 0.8 mmol g^{-1}, 1.6 mmol g^{-1}, and 3.2 mmol g^{-1}; Pb/Sn = 1 : 1) were prepared following the method described above. These samples were denoted as Pb–Sn-beta-1, Pb–Sn-beta-2, Pb–Sn-beta-3, Pb–Sn-beta-4, and Pb–Sn-beta-5. The beta zeolite containing lead alone was denoted as Pb-beta, and the beta zeolite modified with tin alone was denoted as Sn-beta.

2.3 Catalyst characterization

The contents of silicon, aluminum, lead and tin in the catalysts were determined by inductively coupled plasma optical emission spectroscopy (ICP-OES, Perkin Elmer Optima 2100 DV). The powder X-ray diffraction (XRD) data were obtained on a Bruker D8 Advance X-ray powder diffractometer (40 kV, 40 mA, CuKα radiation of 1.54 Å) to characterize the crystal structures over a 2θ range of 10° to 70° at room temperature. The nitrogen adsorption–desorption experiment was performed using a Micromeritics ASAP2020M analyzer at −196 °C. The specific surface area (S_{BET}) was calculated with the Brunauer–Emmett–Teller (BET) method over a range of relative pressures from 0.005 to 0.25. The pore-size distribution was derived from the desorption branches of the isotherms using the Barrett–Joyner–Halenda (BJH) method and the total pore volume (V_{total}) was estimated at a relative pressure (P/P_o) of approximately 0.99. The X-ray photoelectron spectra (XPS) of dehydrated samples were carried out using PHI-5000C ESCA system with Al Kα radiation ($h\nu$ = 1486.6 eV).

The total acidity of the catalysts was obtained by NH_3 temperature-programmed desorption (TPD) using a Micromeritics AutoChemII 2920. The 100 mg catalyst was pretreated in helium at 300 °C for 1 h, after which the catalyst was cooled to 120 °C in a helium flow. Subsequently, 5% ammonia in the helium flow was absorbed on catalyst at 120 °C for 2 h, and then the dry helium flow was used to remove the weakly adsorbed ammonia. Finally, NH_3-TPD was performed from 120 °C to 800 °C at the ramp of 10 °C min^{-1} in the dry helium flow.

FT-IR spectra of the adsorbed pyridine studied the acidic properties of samples. In the measurement, each sample (10 mg) was pressed into a self-supported wafer with a diameter of 13 mm. The wafer was placed in a quartz IR cell sealed with CaF_2 windows and connected to a vacuum system, in which the samples were dried at 450 °C for 2 h under vacuum and then cooled to room temperature. Subsequently, the wafer was exposed to pyridine vapour and allowed to adsorb pyridine for 30 min. Finally, the desorption step at 150 °C (60 min) was performed.

2.4 Reaction tests and product analysis

All catalytic reactions were performed in a stainless steel autoclave with a closed Teflon vessel (50 ml). In a typical experiment,

the vessel was charged with carbohydrate (7.5 mmol C), catalyst (200 mg) and water (10 ml), and the autoclave was heated to 190 °C in a rotating oven (20 rpm). Once the set temperature was attained, the reactor was held at that temperature for 2 h, after which the autoclave was quenched in a cold bath. Finally, the reaction mixture was separated by centrifugation, while the supernatant liquid was diluted with deionized water before analysis.

The concentration of sugars, organic acids (*i.e.* lactic acid, glycolic acid, formic acid and acetic acid) and 5-hydroxymethylfurfural was analyzed on an Agilent 1200 series HPLC (Bio-Rad HPX-87H) with a RI and UV detector (210 nm) using a 5 mM aqueous sulphuric acid solution as the eluent at a flow rate of 0.5 ml min^{-1}. The column and RI detector temperature were set at 55 °C and 45 °C, respectively. All products were determined based on the external standard. The conversion of sugars and the yield of products were determined based on carbon as follows:

$$\text{Sugar conversion } (C\%) = \left(1 - \frac{\text{moles of unconverted sugar}}{\text{moles of initial sugar}}\right) \times 100\%$$

$$\text{Product yield } (C\%) = \frac{\text{moles of carbon in phase product}}{\text{moles of carbon in initial sugar}} \times 100\%$$

3. Results and discussion

3.1 Catalytic performance of different bimetal modified beta zeolites

The transition metals (Ni and Cu), lanthanide (Ce) and primary group element (Pb) were selected to modify Sn-beta zeolite catalysts for conversion glucose into lactic acid. The results indicated that Sn-beta zeolite catalysts containing different metal species exhibited significant difference catalytic activities for production of lactic acid (Table S1†). The median LA and high HMF yield together with a small amount of formic acid, acetic acid and glycolic acid were generated using Ni–Sn-beta, Cu–Sn-beta or Ce–Sn-beta catalyst. The high LA and low HMF yields were obtained over Pb–Sn-beta. The conversions were all greater than 99% for all catalysts. Hence, Pb–Sn-beta zeolite catalyst was selected to further evaluate the catalytic activity of conversion glucose to lactic acid.

3.2 Catalytic performance of lead and tin modified catalysts for glucose conversion

The results of glucose conversion into lactic acid using different catalysts are shown in Fig. 1. A negligible yield of LA was obtained without adding catalyst. In the presence of the beta, the yield of LA was low, approximately 6%, and the main product was HMF with a yield of 15%, together with a small amount of formic acid, acetic acid and glycolic acid. The result can be explained to internal Brønsted and Lewis acids of the beta
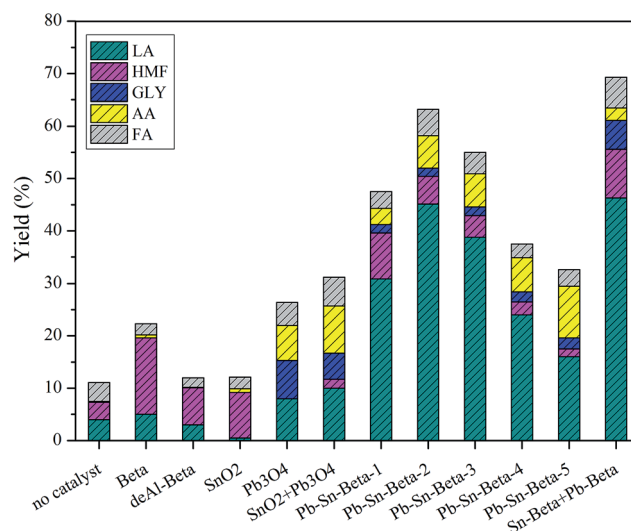

Fig. 1 Comparison of different catalysts for the conversion of glucose. Reaction conditions: 190 °C, 2 h, air, 225 mg glucose and 200 mg catalyst. LA: lactic acid, AA: acetic acid, FA: formic acid, and GLY: glycolic acid. Metal content of Sn-beta + Pb-beta: Sn = 0.2 mmol g^{-1}, Pb = 0.2 mmol g^{-1}.

zeolite.[42] The yields of LA and HMF decreased, when deAl-beta was used as a catalyst, especially HMF. This result occurred due to the decreasing acidity of deAl-beta. In the case of SnO$_2$, Pb$_3$O$_4$ and SnO$_2$ + Pb$_3$O$_4$, low yields of LA were generated, indicating they do not affect lactic acid synthesis. However, when beta zeolite containing lead and tin (Pb–Sn-beta-1) was used, the yield of LA dramatically increased to approximately 39%, whereas the yield of HMF was only 9%. The yields of LA initially increased and then decreased with further increases in lead and tin loading. As the contents of lead and tin exceeded 0.8 mmol g^{-1} (Pb–Sn-beta-3), the yields of LA sharply declined, implying an abrupt change of catalyst properties. Moreover, the catalytic performance of Sn-beta + Pb-beta was investigated to clarify the effect of the metal located sites in beta zeolites on products yields. The result indicated that located sites of lead and tin have no effect on LA yield, because Sn-beta + Pb-beta (0.4 mmol g^{-1}) and Pb–Sn-beta-2 (0.4 mmol g^{-1}) have comparable LA yield. The maximum yield of LA was up to 45% within the loading scope of lead and tin of 0.2–0.4 mmol g^{-1}. It was well accepted that Brønsted acid sites can catalyze the hydrolysis of monosaccharide,[43] and Lewis acid sites can catalyze the isomerization of glucose to fructose, followed by retro-aldol condensation and a series of isomerization reactions to lactic acid.[44] Based on this theory, we speculate that appropriate loading of lead and tin tunes the acidity of the beta zeolite, generating great potential for glucose conversion and lactic acid production. To confirm the hypothesis, the physicochemical properties, structures and acidity of beta zeolites with different lead and tin contents were explored.

3.3 Textural properties and XRD

The results of the textural properties determined by nitrogen physisorption were showed in Table 1. The raw beta zeolite had

Table 1 Physicochemical properties of catalysts

Catalyst	S_{BET} (m^2 g^{-1})	V_{total} (ml g^{-1})	$V_{micropore}$ (ml g^{-1})	Pb^a (mmol g^{-1})	Sn^a (mmol g^{-1})	Si/Al^a ratio
Beta	585.0	0.345	0.188	—	—	25
deAl-beta	578.5	0.365	0.189	—	—	>1700
Pb–Sn-beta-1	576.0	0.358	0.183	0.08	0.11	>1700
Pb–Sn-beta-2	573.7	0.351	0.179	0.19	0.21	>1700
Pb–Sn-beta-3	533.0	0.320	0.167	0.38	0.41	>1700
Pb–Sn-beta-4	441.4	0.293	0.137	0.81	0.79	>1700
Pb–Sn-beta-5	323.9	0.205	0.103	1.62	1.61	>1700
Pb–Sn-beta$^{1th b}$	574.0	0.362	0.189	0.15	0.16	>1700
Pb–Sn-beta$^{2th c}$	577.4	0.402	0.184	0.09	0.15	>1700

^{a} Determined by ICP-OES analysis. ^{b} Catalyst after first calcination. ^{c} Catalyst after second calcination.

a BET surface area of 585.0 m^2 g^{-1}, total pore volume of 0.345 ml g^{-1} and micropore volume of 0.188 ml g^{-1}. Dealumination of beta zeolite decreased the BET surface area (578.5 m^2 g^{-1}) and increased total pore volume (0.365 ml g^{-1}). The reason was that dealumination resulted in mesopore generation and increase the average pore diameter. With the lead and tin incorporation into beta zeolites (Pb–Sn-beta-1, Pb–Sn-beta-2, Pb–Sn-beta-3), the BET surface areas and pores volumes decreased. The observed decrease of BET surface areas and accessibility of the pores may be caused by occupation of channels or opening pores from metal species. As contents of lead and tin species exceeded 0.8 mmol g^{-1} (Pb–Sn-beta-3) in beta zeolite, the BET surface areas, total pore volumes and micropore volumes evidently decreased from 533.0 to 323.9 m^2 g^{-1}, 0.320 to 0.205 ml g^{-1} and 0.167 to 0.103 ml g^{-1}, respectively. This was ascribed to the pores blocked from lead and tin over-loading, which corresponding to the inferior catalytic activity for glucose conversion into lactic acid.

X-ray diffraction patterns of the samples are shown in Fig. 2. Compared to the raw beta zeolite, dealumination with HNO$_3$ did not affect the phase structure, which suggests that the framework of deAl-beta remained fully intact. Besides, deAl-beta zeolite possessed a high ratio of Si/Al (>1700) introducing an amount of vacant framework sites, which would be able to be occupied by incorporated metal species.[41,45] The d-spacing can

be used to inspect the change of unit cell volume induced by incorporation of lead and tin species. Using calculated d_{302} (2θ = 22.4–22.5°) of raw beta and deAl-beta suggested that there was a contraction ($\pm$3.977–3.930 Å) in the unit cell volume of deAl-beta zeolite. With the lead and tin incorporation into deAl-beta zeolite, the unit cell volume had a slight re-expansion (3.972 Å for Pb–Sn-beta-1 and Pb–Sn-beta-2, 3.956 Å for Pb–Sn-beta-3); however, no obvious changes were observed in the typical diffraction pattern. This result indicated that vacant framework sites were occupied upon incorporation of lead and tin species. In addition, there was a complete absence of any SnO$_2$ and Pb$_3$O$_4$ reflections, suggesting that either other amorphous metal oxide (Sn$_x$O$_y$ and Pb$_x$O$_y$) existed or SnO$_2$ and Pb$_3$O$_4$ highly dispersed in the zeolites pores. The results were in accordance with previous studies, which reported metal oxides might be non-crystalline phase or good dispersion when the metal content was low.[41,46,47] However, with metal species contents beyond 0.8 mmol g^{-1} in beta zeolite (Pb–Sn-beta-3), further increased contents of lead and tin drastically decreased intensities of the typical peak (14.5°, 22.5° and 30.0°), which may be ascribed to partial loss of crystallinity resulting from metal species over-loading. Moreover, the SnO$_2$ and Pb$_3$O$_4$ produced a very clear diffraction peaks (26.3°, 26.7°, 33.9°, 52.0° and 51.8°) in beta zeolites, indicating that extraframework metal oxides generated with metal species contents beyond 0.8 mmol g^{-1} during calcinations. And the peaks intensities of corresponding oxides increased with increasing metal species content, which were all corresponding to the inferior catalytic activity. The reason was that SnO$_2$ and Pb$_3$O$_4$ had a negligible catalytic activity for glucose conversion into lactic acid, and amounts of metal oxides covered the catalytic activity sites.
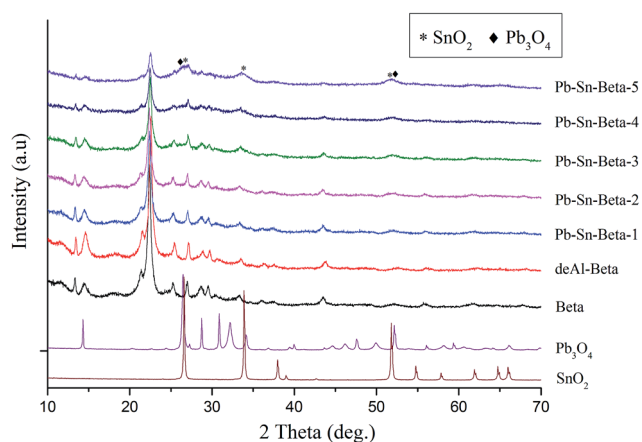
3.4 States of Sn and Pb in beta zeolites

The XPS curves of tin and lead are showed in Fig. 3. The binding energies (BEs) of the elements were calibrated with respect to the C 1s peak at 284.6 eV. The Sn 3d XPS spectra exhibited two distinct Sn 3d$_{5/2}$ and Sn 3d$_{3/2}$ states at 487.7 and 496.2 eV, respectively in different catalysts, which would be attributed to tetrahedrally coordinated framework Sn species. However, the 3d$_{5/2}$ and 3d$_{3/2}$ binding energy values of extra-framework Sn species positioned at 486.0 and 494.4 eV, which is characteristic of octahedral Sn species.[48,49] The results were corresponding to
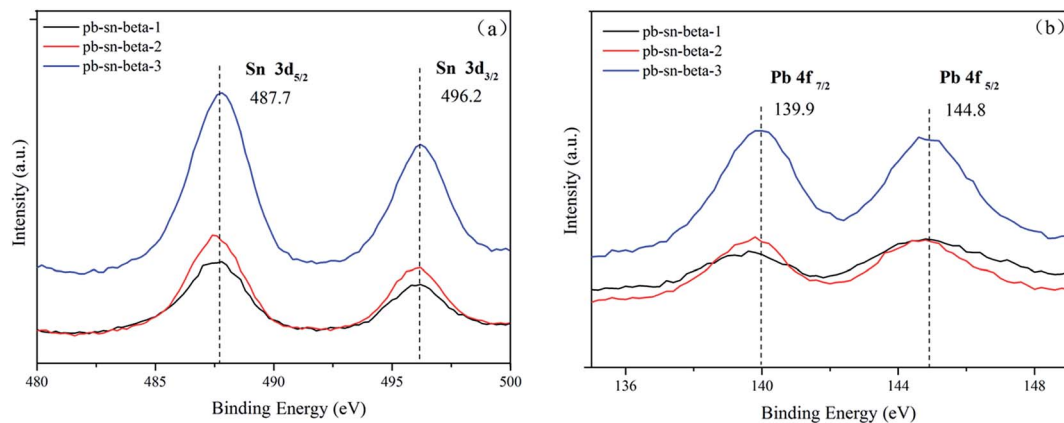

Fig. 2 X-ray diffraction patterns of various catalysts.

Fig. 3   XPS spectra of the Sn 3d and Pb 4f states of different catalysts.

that of Bo Tang *et al.*,[50] while also indicated that tin was incorporated into the framework of catalyst. In the Pb 4f region, the signals appeared at binding energy for Pb $4f_{7/2}$ of 139.9 eV, which was greater than the binding energy of pure Pb_3O_4 (137.9 eV), indicating that lead did not exist as extra-framework Pb species. The XPS results revealed that tin and lead species were coordinated in BEA framework with low metal loading (below 0.8 mmol g^{-1}). The results were accordance with the results from the nitrogen physisorption and XRD.

3.5   Acidity

The NH_3-TPD pattern of each catalyst is depicted in Fig. 4. The large and medium desorption peak of raw beta zeolite centered at approximately 200 °C and 320 °C indicated that it had weak and medium acid sites. In the case of deAl-beta zeolite, the weak and medium acidic site accordingly disappeared following the removal of Al from the raw beta zeolite. However, the surface acidity was significantly changed with the incorporation of lead

and tin into the framework of the deAl-beta zeolite. With metal species loading below 0.8 mmol g^{-1} (Pb–Sn-beta-3), the samples presented two desorption peaks at approximately 160 °C and 600 °C that, respectively, corresponding to weak and strong acid sites. With increased lead and tin loads, the strong acid sites gradually decreased, whereas the weak acid sites increased. However, as metal species loading exceeded 0.8 mmol g^{-1}, the samples were dominated by weak acid sites.

To distinguish Lewis and Brønsted acid sites, the IR spectra of various catalysts adsorbing pyridine are shown in Fig. 5. The peaks at approximately 1449 cm^{-1} and 1540 cm^{-1} were assigned to Lewis acid sites and Brønsted acid sites, respectively. The peak at 1490 cm^{-1} was attributed to pyridine absorbed on both Lewis and Brønsted acid sites (B + L). Following the raw beta zeolite was treated with HNO_3, the peak at 1540 cm^{-1} and 1490 cm^{-1} disappeared, and the peak at 1449 cm^{-1} decreased in intensity. As lead and tin were incorporated into the deAl-beta zeolite, the Brønsted acid sites were still absent, while the Lewis acid sites gradually increased with increasing metal
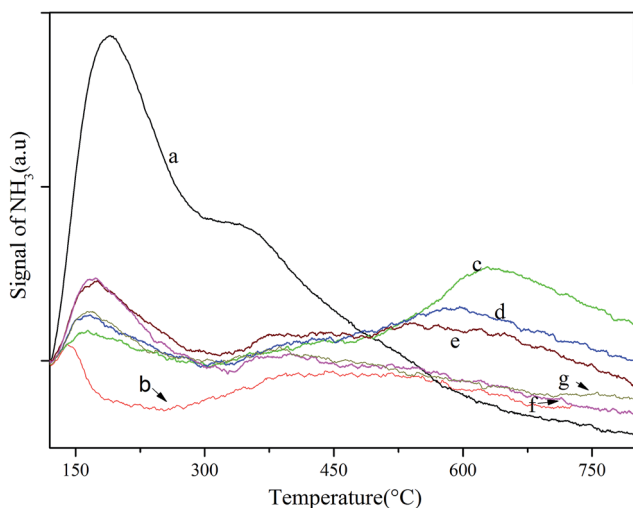

Fig. 4 NH_3-TPD curves of various catalysts: (a) beta; (b) deAl-beta; (c) Pb–Sn-beta-1; (d) Pb–Sn-beta-2; (e) Pb–Sn-beta-3; (f) Pb–Sn-beta-4; and (g) Pb–Sn-beta-5.
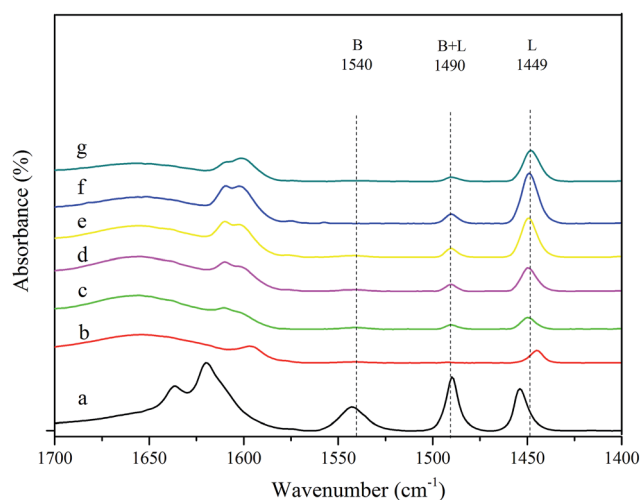

Fig. 5   FTIR spectra following the adsorption of pyridine on various catalysts: (a) beta; (b) deAl-beta; (c) Pb–Sn-beta-1; (d) Pb–Sn-beta-2; (e) Pb–Sn-beta-3; (f) Pb–Sn-beta-4; (g) Pb–Sn-beta-5.

species loading (curves c–f). Although the Pb–Sn-beta-3 and Pb–Sn-beta-4 had more Lewis acid sites than Pb–Sn-beta-2, the catalytic performance of Pb–Sn-beta-2 was superior to that of both. Coincidentally, research has indicated that catalyst with excess Lewis acidity form humins from glucose.[47] We also found that higher Lewis acid sites increased the yield of humins, while the LA yield was lower. Therefore, the catalyst with appropriate Lewis and Brønsted acid sites seemed suitable for lactic acid production. The contents of Lewis and Brønsted acid sites of different catalysts are shown in Table S2.†

3.6 Catalyst reusability

To make uttermost use of catalysts, the reusability of the Pb–Sn-beta zeolite in the conversion glucose into lactic acid was investigated. First, catalysts were recovered by centrifugation and separation after the first trial, dried at 70 °C overnight, and then calcined at 550 °C to run again under identical reaction conditions. The catalytic activity results of reusable catalysts are presented in Fig. S1.† The glucose conversion decreased from 99% to 87% and LA yield dropped from an initial value of 52% to 33% over the course of three recycling trials. In contrast, the yield of HMF increased, indicating that the catalytic characteristics of Pb–Sn-beta might be changed in the process of recycling trials. To further explore the reasons for catalyst deactivation, the used catalyst was characterized by XRD (Fig. S2†), nitrogen physisorption analysis (Table 1) and pyridine FT-IR (Table S2†). The results of the XRD pattern analysis revealed that used Pb–Sn-beta did not have difference in phase characteristics, compared with the fresh catalyst. The nitrogen physisorption analysis showed that S_{BET}, V_{micro} and V_{total} of the second calcined catalyst increased to $577.4 \ m^2 \ g^{-1}$, $0.184 \ ml \ g^{-1}$ and $0.402 \ ml \ g^{-1}$, respectively, compared with fresh catalyst. This could be ascribed to leaching of metal species and formation of a great number of mesoscopic pores. Moreover, pyridine FTIR analysis indicated that Lewis acid sites gradually decreased, while Brønsted acid sites were almost unchanged with used times. Lewis acidity was decreased because metal species were leached. The result was also confirmed by ICP-OES analysis (Table 1), which showed that the contents of lead and tin decreased to $0.09 \ mmol \ g^{-1}$ and $0.15 \ mmol \ g^{-1}$ after the second calcination. The changes in Lewis and Brønsted acid sites obviously affected the products distribution. Due to relatively increased Brønsted to Lewis acid sites ratio, the dehydration step of monosaccharide to HMF was promoted, and the conversion step of intermediates from monosaccharide dissociation to lactic acid was inhibited. Hence, the observed decrease in catalytic performance during recycling mainly could be due to the leaching of metal species. This indicated that the stability of the Pb–Sn-beta catalyst prepared by the solid-state ion-exchange method still needs to be improved.

3.7 Conversion of other biomass over Pb–Sn-beta

The various biomass materials, including monosaccharides (fructose, glucose and mannose), disaccharides (sucrose and lactose) and polysaccharides (starch and cellulose), were hydrothermally converted over the Pb–Sn-beta zeolite, as shown in Table S3.† The monosaccharides were completely converted, and the lactic acid yields showed no significant difference, as they all obtained yields greater than 50%. The disaccharides were also completely converted, but the LA yield was much different. The sucrose, consisting of one fructose and one glucose unit, and the lactose, consisting of one glucose and one galactose unit, yielded 51.2% and 37.8% LA, respectively. The results suggested that catalytic conversion of sucrose and lactose may proceed *via* a different reaction route. When starch and cellulose were used as feedstock, which are polysaccharides consisting of a large number of glucose units, conversion of both were approximately 30%, and lactic acid yields decreased to 10.1% and 16.2%, respectively. These results indicated that depolymerization of polysaccharides might need higher temperature and longer reaction time than present reaction condition (190 °C and 2 h) or that Pb–Sn-beta catalyst might not have catalytic activity for conversion cellulose and starch into lactic acid. In the future work, we will change the reaction condition or catalyst to improve the yield of lactic acid from polysaccharides.

3.8 Effect of reaction conditions on the conversion of glucose over Pb–Sn-beta

To achieve the maximize LA yield, a series of reaction conditions were evaluated. The Fig. S3† depicts the effect of different catalyst dosages on products yields and the conversion of glucose. The LA yield increased before the catalyst dosage reached 200 mg and the mass ratio of catalyst to glucose was 0.9. As the catalyst dosage exceeded 200 mg, the LA yield was almost invariable and reached a plateau at approximately 50%. Conversely, HMF yield consistently decreased with increasing catalyst dosage. The yield of other products was nearly unchanged in the range of catalyst dosage from 40 to 280 mg. When the catalyst dosage was chosen to be 200 mg, the products yields as a function of reaction temperature are described in Fig. S4.† The LA yields increased sharply as the reaction temperature increased from 150 °C to 190 °C, and they slightly declined beyond 190 °C. The yields of other products (HMF, FA, and GLY) also presented the same trend. The highest LA yield of 52% was obtained when the reaction time was 2 h at 190 °C, as shown in Fig. S5.† The LA yield varied little when the reaction time exceeded 2 h. In contrast, HMF yield gradually decreased with increased reaction times. The results suggested that HMF decomposed to other products at longer reaction times. The yield of other products, such as FA, GLY, AA, and Ox, varied slightly at prolonged reaction times.

Atmosphere condition also dramatically influenced product yields. Three kinds of atmosphere condition (air, nitrogen and oxygen) under ambient pressure were investigated (Fig. S6†). As the catalyst dosage, temperature and time were fixed, the yields of LA were largest in air, followed by in N_2 and then, in O_2. The yield of HMF exhibited also similar order. The highest yields of LA were achieved in ambient pressure air, which was convenient, safety and lower energy consumption to producing lactic acid in industrial process.

The effects of the lead to tin molar ratio on the yields of products are shown in Fig. 6. The conversion of glucose was higher than 98% in all cases. As the Pb/Sn molar ratio was approximately from 3/7 to 4/6, the maximum LA yield was generated. The LA yield gradually decreased with Pb/Sn molar ratios beyond 4/6. The HMF yield was nearly invariable for different lead to tin molar ratios (3/7–7/3). However, HMF had the highest yield over beta zeolite containing tin alone (Sn-beta) and lowest yield over beta zeolite containing lead alone (Pb-beta). Other main products including FA, AA, GLY had a relatively lower yield compared with LA yield. Apparently, the lead to tin molar ratio had a pronounced effect on the products distribution. The yield of LA was closed to 52% together with 6.4% HMF, 2.8% AA, 4.8% FA and 1.2% GLY at the lead to tin molar ratio of 4/7. However, when the lead to tin molar ratio was 0/10 or 10/0, the LA yield was 26.8% or 26.5%, respectively, which was far lower than the 52% LA yield. These results indicated that lead and tin incorporated into beta zeolite had a strong synergistic effect on the conversion of glucose to lactic acid. The ICP results of different Pb/Sn molar ratio are shown in Table S4.†

3.9 Reaction mechanism and catalytic synergistic function of lead and tin

It was well accepted that Lewis acids can promote the isomerization of glucose to fructose.[51,52] In this process, many studies have proposed that the hydrolyzed framework tin species in Sn-beta zeolite were responsible for the isomerization of glucose to fructose; moreover, ^{13}C NMR and ^{1}H NMR studies confirmed the isomerization process by 1, 2-H shift.[51] In addition, Pb(II)–OH species in aqueous also demonstrated the key role for isomerization of glucose to fructose.[28] We speculate that the reaction pathway for the conversion of glucose into lactic acid over the Pb–Sn-beta zeolite begins with isomerization of glucose to fructose via 1, 2-H shift by a cooperative interaction with lead

and tin. Subsequently, Lewis acids catalysts facilitate the retro-aldol condensation of fructose to produce two C3 intermediates (that is glyceraldehyde and dihydroxyacetone), and then glyceraldehyde and dihydroxyacetone may undergo dehydration to 2-hydroxypropenal that produce pyruvaldehyde via keto–enol tautomerization. Finally the pyruvaldehyde isomerizes into lactic acid by Lewis acid facilitating the nucleophilic attack of the electron donor to the carbonyl functional group of the aldehyde, thereby completing intramolecular rearrangement by the shift of hydride. For this complex cascade reaction, many studies have demonstrated that Sn-beta plays a key role as a Lewis acid; in addition, Wang et al. applied theoretical calculations to show the positive effect of lead(II) species on this process.[28,31,44] Therefore, we speculate that lead and tin species cooperatively interact in this complex cascade.

To verify the above hypothesis regarding the reaction pathway and to explore synergistic effects of lead and tin in the catalytic reaction, the key intermediates (fructose, dihydroxyacetone, glyceraldehyde and pyruvaldehyde) were used as the probe reactants that were catalyzed by Pb-beta, Sn-beta, and Pb–Sn-beta zeolites, respectively. The results with glucose, fructose, dihydroxyacetone, glyceraldehyde, and pyruvaldehyde as a function of time are shown in Fig. S7.† In the reaction of glucose, the reaction rate was much faster, and the LA yield was higher over Pb–Sn-beta zeolite than over the Sn-beta or Pb-beta zeolites. The yield of LA was 26.5%, 22.4% and 52% over Pb-beta, Sn-beta and Pb–Sn-beta zeolites, respectively, for 120 min. A similar trend was found when using fructose as the feedstock. The yield of LA was 20%, 40% and 55% using Pb-
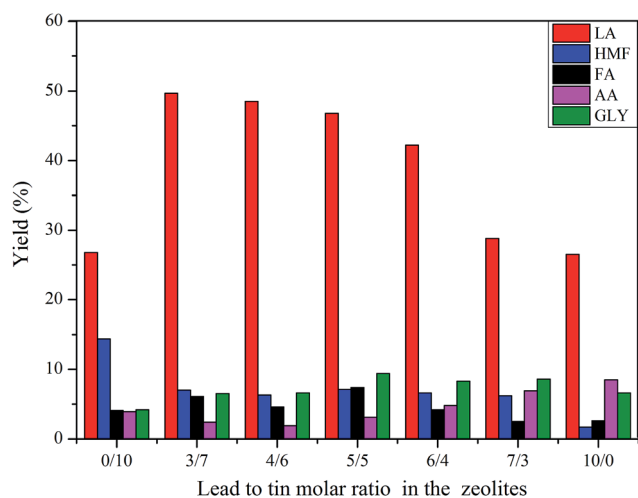
Fig. 6 Effect of the lead to tin molar ratio on the yields of main products with Pb–Sn-beta reaction conditions: 190 °C, 2 h, air, 225 mg glucose and 200 mg catalyst (0.3 mmol g^{-1} metal loading). LA: lactic acid, AA: acetic acid, FA: formic acid, and GLY: glycolic acid.

Table 2 Conversion of different carbohydrates as the probe reactants over different beta zeolites^a

Entry	Feedstock	Catalyst	The yield of aqueous-phase products (%)				
			LA	HMF	AA	FA	GLY
1	Glucose	Pb–Sn-beta	52.0	6.4	2.8	4.8	1.2
2	Glucose	Pb-beta	26.5	3.6	8.5	2.6	6.6
3	Glucose	Sn-beta	22.4	14.4	3.9	4.1	4.2
4	Glucose	—	0.4	6.7	—	—	—
5	Fructose	Pb–Sn-beta	54.6	4.3	6.7	5.9	6.2
6	Fructose	Pb-beta	20.6	2.5	13.3	6.5	5.2
7	Fructose	Sn-beta	40.0	13.5	—	—	—
8	Fructose	—	17.4	43.9	—	1.7	1.7
9	Dihydroxyacetone	Pb–Sn-beta	70.0	—	7.5	2.3	—
10	Dihydroxyacetone	Pb-beta	17.7	—	5.5	3.5	4.3
11	Dihydroxyacetone	Sn-beta	95.6	—	—	—	—
12	Dihydroxyacetone	—	21.1	—	30.9	5.8	—
13	Pyruvaldehyde	Pb–Sn-beta	69.0	—	9.2	1.9	—
14	Pyruvaldehyde	Pb-beta	37.0	—	21.2	2.6	—
15	Pyruvaldehyde	Sn-beta	76.0	—	11.5	3.3	—
16	Pyruvaldehyde	—	26.5	—	24.8	2.5	—
17	Glyceraldehyde	Pb–Sn-beta	56.5	6.6	6.2	2.2	2.3
18	Glyceraldehyde	Pb-beta	28.9	3.2	11.6	5.0	26.7
19	Glyceraldehyde	Sn-beta	81.3	11.0	—	9.0	—

^{a} Reaction conditions: 190 °C, 2 h, air, 10 ml water, 225 mg carbohydrate (7.5 mmol), 200 mg catalyst (Pb–Sn-beta: 0.3 g^{-1} metal loading, Pb/Sn ratio = 4/7; Sn-beta and Pb-beta: 0.3 mmol g^{-1} metal loading).

beta, Sn-beta and Pb–Sn-beta zeolites, respectively, for 120 min. Clearly, compared with the reaction of glucose, the LA yield from fructose dramatically increased over Sn-beta zeolite, whereas it remained nearly constant over Pb-beta zeolite. The result implied that the isomerization of glucose to fructose was an obstacle for producing lactic acid over the Sn-beta zeolite.
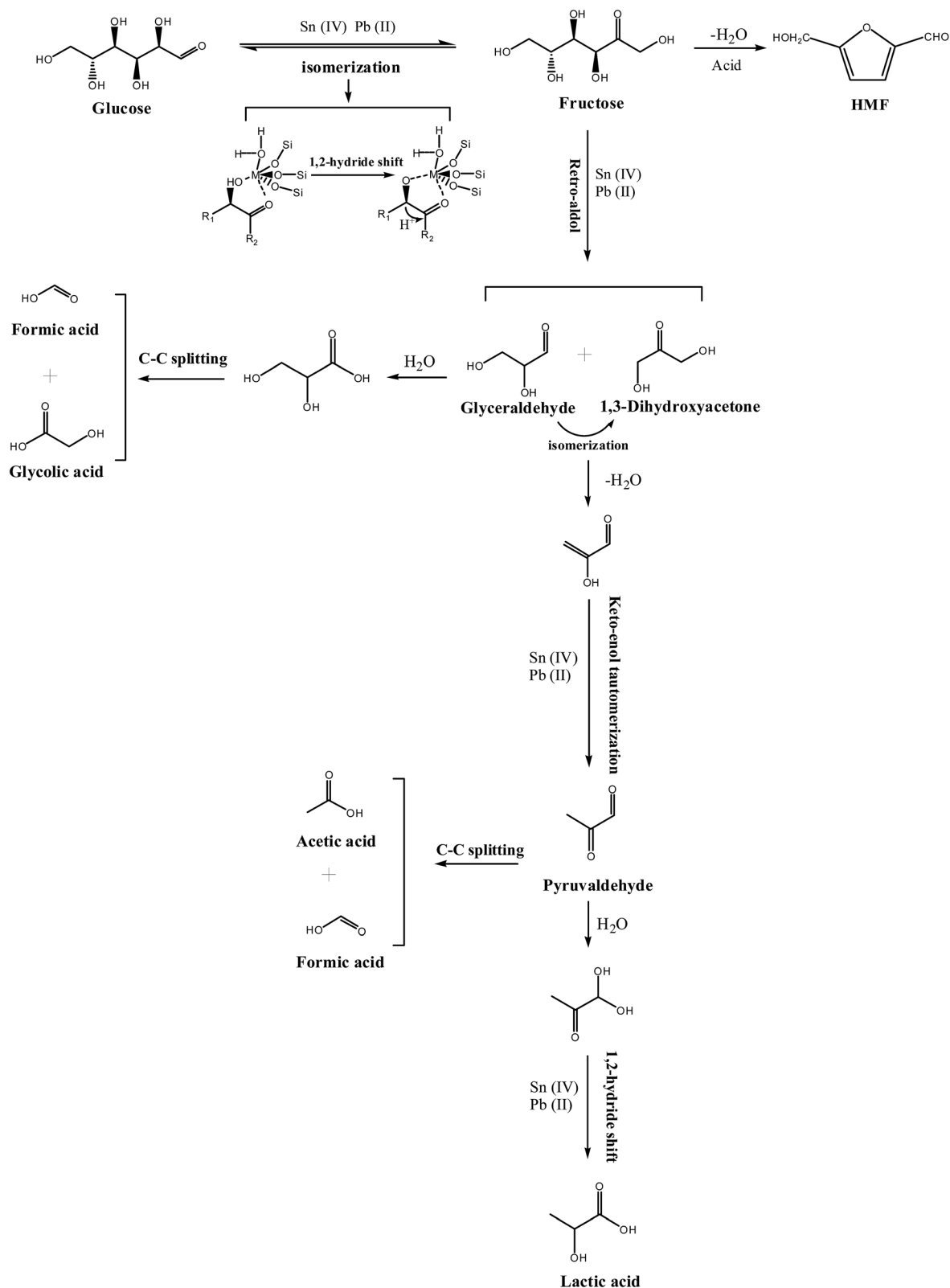
Scheme 1 Proposed reaction mechanism for the conversion of glucose to lactic acid over Pb−Sn-beta.

However, the Pb–Sn-beta zeolite is advantageous in the isomerization reaction, because the LA yield from fructose was nearly the same as that from glucose. Therefore, incorporating lead into the Sn-beta zeolite improves ability of isomerization of glucose to fructose compared to that over Sn-beta zeolite.

Moreover, in the reaction of dihydroxyacetone, the yield of LA reached 80% and 70% over Sn-beta and Pb–Sn-beta, respectively, for only 60 min, after which the yield maintained almost invariant. Compared with the reaction of fructose, the LA yield was observably increased by Sn-beta; however, the LA yield was nearly same as that from fructose, approximately 20% over Pb-beta in 120 min. Therefore, the retro-aldol condensation of fructose to produce two C3 intermediates has a clear obstacle over Sn-beta, and the incorporation of lead into Sn-beta decreased the effect of that obstacle. Hence, lead affects the retro-aldol condensation from fructose to C3 intermediates more than tin. For the reaction of pyruvaldehyde, the LA yield was 70% and 68% using Sn-beta and Pb–Sn-beta, respectively, in only 30 min, after which the yield achieved a plateau. The LA yield was 37% in 120 min by Pb-beta. Apparently, compared with reaction of dihydroxyacetone, the LA yield was nearly invariant with beta zeolite containing tin (Sn-beta and Pb–Sn-beta), which implied that tin exhibited dramatically efficiency on the conversion of dihydroxyacetone or pyruvaldehyde to lactic acid. Thus, it is very likely that tin species have a greater influence on the dehydration of dioxyacetone and the isomerization of pyruvaldehyde, which are key steps in the conversion of sugar into lactic acid.

The yield of main by-products was also investigated to explore the effect of inhibition of lead and tin on the distribution of products (Table 2). For the reaction of glucose and fructose, the HMF yield was lower over the catalysts containing lead, such as Pb-beta or Pb–Sn-beta zeolite than over Sn-beta zeolite, and it was the lowest over the Pb-beta zeolite. Therefore, the other key role of lead was advantageous of inhibition primary by-product HFM. Other side-products (*i.e.*, AA, FA and GLY) were produced by glyceraldehyde that proceeded *via* a cascade reaction to produce glycolic acid and formic acid, or by pyruvaldehyde that formed formic acid and acetic acid *via* C–C splitting. However, these side-products were low yields on the glucose reaction. In a word, lead and tin in the Pb–Sn-beta zeolite acted as Lewis acid to synergistically promote a series of complex reactions to produce lactic acid; in this process, lead played a more key role in the isomerization of glucose to fructose and the retro-aldol condensation from fructose to C3 intermediates, whereas tin promoted the dehydration of dioxyacetone and the isomerization of pyruvaldehyde. In addition, lead has a positive effect on inhibition primary by-product, HMF. The summarized reaction mechanism is shown in Scheme 1.

4. Conclusion

An efficient synthesis of lactic acid from sugars in aqueous phase was achieved using Pb–Sn-beta zeolite prepared by solid-state ion-exchange method. Under the optimum reaction conditions, the highest lactic acid yield was 52% from glucose.

A synergistic effect of lead and tin on the conversion of glucose to lactic acid was discovered. The key role of lead was isomerization reaction from glucose to fructose and the retro-aldol condensation from fructose to C3 intermediates, while tin had a superior catalytic performance in the dehydration of dihydroxyacetone and isomerization of pyruvaldehyde. In addition, lead had a positive effect on inhibition mainly by-product HMF.

Conflicts of interest

There are no conflicts to declare.

Acknowledgements

References

1 D. M. Alonso, J. Q. Bond and J. A. Dumesic, Catalytic conversion of biomass to biofuels, *Green Chem.*, 2010, **12**, 1493–1513.

2 P. Gallezot, Conversion of biomass to selected chemical products, *Chem. Soc. Rev.*, 2012, **41**, 1538–1558.

3 B. O. de Beeck, M. Dusselier, J. Geboers, J. Holsbeek, E. Morré, S. Oswald, L. Giebeler and B. F. Sels, Direct catalytic conversion of cellulose to liquid straight-chain alkanes, *Energy Environ. Sci.*, 2015, **8**, 230–240.

4 M. Dusselier, P. Van Wouwe, A. Dewaele, E. Makshina and B. F. Sels, Lactic acid as a platform chemical in the bio based economy: the role of chemocatalysis, *Energy Environ. Sci.*, 2013, **6**, 1415.

5 P. Maki-Arvela, I. L. Simakova, T. Salmi and D. Y. Murzin, Production of lactic acid/lactates from biomass and their catalytic transformations to commodities, *Chem. Rev.*, 2014, **114**, 1909–1971.

6 X. Zhang, L. Lin, T. Zhang, H. Liu and X. Zhang, Catalytic dehydration of lactic acid to acrylic acid over modified ZSM-5 catalysts, *Chem. Eng. J.*, 2016, **284**, 934–941.

7 Z. Huo, J. Xiao, D. Ren, F. Jin, T. Wang and G. Yao, Chemoselective synthesis of propionic acid from biomass and lactic acid over a cobalt catalyst in aqueous media, *Green Chem.*, 2017, **19**, 1308–1314.

8 P. i. Mäki-Arvela, I. L. Simakova, T. Salmi and D. Y. Murzin, Production of lactic acid/lactates from biomass and their catalytic transformations to commodities, *Chem. Rev.*, 2013, **114**, 1909–1971.

9 R. Datta and M. Henry, Lactic acid: recent advances in products, processes and technologies—a review, *J. Chem. Technol. Biotechnol.*, 2006, **81**, 1119–1129.

10 M. A. Abdel-Rahman, Y. Tashiro and K. Sonomoto, Recent advances in lactic acid production by microbial fermentation processes, *Biotechnol. Adv.*, 2013, **31**, 877–902.

11 Y. Wang, Y. Tashiro and K. Sonomoto, Fermentative production of lactic acid from renewable materials: recent achievements, prospects, and limits, *J. Biosci. Bioeng.*, 2015, **119**, 10–18.

12 G.-X. Qi, L. Xiong, C. Huang, X.-F. Chen, X.-Q. Lin and X.-D. Chen, Solvents Production from a Mixture of Glucose and Xylose by Mixed Fermentation of Clostridium Acetobutylicum and Saccharomyces Cerevisiae, *Appl. Biochem. Biotechnol.*, 2015, **177**, 996–1002.

13 B. P. Calabia, Y. Tokiwa and S. Aiba, Fermentative production of l-(+)-lactic acid by an alkaliphilic marine microorganism, *Biotechnol. Lett.*, 2011, **33**, 1429–1433.

14 Y.-J. Wee, J.-S. Yun, D. Kim and H.-W. Ryu, Batch and repeated batch production of L (+)-lactic acid by enterococcus faecalis RKY1 using wood hydrolyzate and corn steep liquor, *J. Ind. Microbiol. Biotechnol.*, 2006, **33**, 431.

15 R. P. John, G. Anisha, K. M. Nampoothiri and A. Pandey, Direct lactic acid fermentation: focus on simultaneous saccharification and lactic acid production, *Biotechnol. Adv.*, 2009, **27**, 145–152.

16 Y. Hayashi and Y. Sasaki, Tin-catalyzed conversion of trioses to alkyl lactates in alcohol solution, *Chem. Commun.*, 2005, 2716–2718.

17 A. Onda, T. Ochi, K. Kajiyoshi and K. Yanagisawa, A new chemical process for catalytic conversion of ᴅ-glucose into lactic acid and gluconic acid, *Appl. Catal., A*, 2008, **343**, 49–54.

18 Z. Huo, Y. Fang, D. Ren, S. Zhang, G. Yao, X. Zeng and F. Jin, Selective conversion of glucose into lactic acid with transition metal ions in diluted aqueous NaOH solution, *ACS Sustainable Chem. Eng.*, 2014, **2**, 2765–2771.

19 X. Yan, F. Jin, K. Tohji, A. Kishita and H. Enomoto, Hydrothermal conversion of carbohydrate biomass to lactic acid, *AIChE J.*, 2010, **56**, 2727–2733.

20 C. A. Ramírez-López, J. R. Ochoa-Gómez, M. a. Fernández-Santos, O. Gómez-Jiménez-Aberasturi, A. Alonso-Vicario and J. Torrecilla-Soria, Synthesis of lactic acid by alkaline hydrothermal conversion of glycerol at high glycerol concentration, *Ind. Eng. Chem. Res.*, 2010, **49**, 6270–6278.

21 Z. Shen, F. Jin, Y. Zhang, B. Wu, A. Kishita, K. Tohji and H. Kishida, Effect of alkaline catalysts on hydrothermal conversion of glycerin into lactic acid, *Ind. Eng. Chem. Res.*, 2009, **48**, 8920–8925.

22 X. Lei, F.-F. Wang, C.-L. Liu, R.-Z. Yang and W.-S. Dong, One-pot catalytic conversion of carbohydrate biomass to lactic acid using an ErCl₃ catalyst, *Appl. Catal., A*, 2014, **482**, 78–83.

23 F.-F. Wang, C.-L. Liu and W.-S. Dong, Highly efficient production of lactic acid from cellulose using lanthanide triflate catalysts, *Green Chem.*, 2013, **15**, 2091–2095.

24 D. Esposito and M. Antonietti, Chemical conversion of sugars to lactic acid by alkaline hydrothermal processes, *ChemSusChem*, 2013, **6**, 989–992.

25 C. Sánchez, L. Serrano, R. Llano-Ponte and J. Labidi, Bread residues conversion into lactic acid by alkaline hydrothermal treatments, *Chem. Eng. J.*, 2014, **250**, 326–330.

26 C. Sánchez, I. Egüés, A. García, R. Llano-Ponte and J. Labidi, Lactic acid production by alkaline hydrothermal treatment of corn cobs, *Chem. Eng. J.*, 2012, **181**, 655–660.

27 S. Zhang, F. Jin, J. Hu and Z. Huo, Improvement of lactic acid production from cellulose with the addition of Zn/Ni/C under alkaline hydrothermal conditions, *Bioresour. Technol.*, 2011, **102**, 1998–2003.

28 Y. Wang, W. Deng, B. Wang, Q. Zhang, X. Wan, Z. Tang, Y. Wang, C. Zhu, Z. Cao and G. Wang, Chemical synthesis of lactic acid from cellulose catalysed by lead(ɪɪ) ions in water, *Nat. Commun.*, 2013, **4**, 2141.

29 K. Nemoto, Y. Hirano, K.-i. Hirata, T. Takahashi, H. Tsuneki, K.-i. Tominaga and K. Sato, Cooperative In–Sn catalyst system for efficient methyl lactate synthesis from biomass-derived sugars, *Appl. Catal., B*, 2016, **183**, 8–17.

30 M. S. Holm, Y. J. Pagán-Torres, S. Saravanamurugan, A. Riisager, J. A. Dumesic and E. Taarning, Sn-beta catalysed conversion of hemicellulosic sugars, *Green Chem.*, 2012, **14**, 702–706.

31 S. Tolborg, I. Sádaba, C. M. Osmundsen, P. Fristrup, M. S. Holm and E. Taarning, Tin-containing Silicates: Alkali Salts Improve Methyl Lactate Yield from Sugars, *ChemSusChem*, 2015, **8**, 613–617.

32 B. Murillo, A. Sánchez, V. Sebastián, C. Casado-Coterillo, O. de la Iglesia, M. P. López-Ram-de-Viu, C. Téllez and J. Coronas, Conversion of glucose to lactic acid derivatives with mesoporous Sn-MCM-41 and microporous titanosilicates, *J. Chem. Technol. Biotechnol.*, 2014, **89**, 1344–1350.

33 B. Murillo, B. Zornoza, O. de la Iglesia, C. Téllez and J. Coronas, Chemocatalysis of sugars to produce lactic acid derivatives on zeolitic imidazolate frameworks, *J. Catal.*, 2016, **334**, 60–67.

34 F. Chambon, F. Rataboul, C. Pinel, A. Cabiac, E. Guillon and N. Essayem, Cellulose hydrothermal conversion promoted by heterogeneous Brønsted and Lewis acids: remarkable efficiency of solid Lewis acids to produce lactic acid, *Appl. Catal., B*, 2011, **105**, 171–181.

35 Y. Wang, F. Jin, M. Sasaki, Wahyudiono, F. Wang, Z. Jing and M. Goto, Selective conversion of glucose into lactic acid and acetic acid with copper oxide under hydrothermal conditions, *AIChE J.*, 2013, **59**, 2096–2104.

36 Q. Guo, F. Fan, E. A. Pidko, V. D. G. Wn, Z. Feng, C. Li and E. J. Hensen, Highly active and recyclable Sn-MWW zeolite catalyst for sugar conversion to methyl lactate and lactic acid, *ChemSusChem*, 2013, **6**, 1352–1356.

37 C. F. De, M. Dusselier, R. R. Van, P. Vanelderen, J. Dijkmans, E. Makshina, L. Giebeler, S. Oswald, G. V. Baron and J. F. Denayer, Fast and selective sugar conversion to alkyl lactate and lactic acid with bifunctional carbon–silica catalysts, *J. Am. Chem. Soc.*, 2012, **134**, 10089.

38 D. Verma, R. Insyani, Y.-W. Suh, S. M. Kim, S. K. Kim and J. Kim, Direct conversion of cellulose to high-yield methyl lactate over Ga-doped Zn/H-nanozeolite Y catalysts in supercritical methanol, *Green Chem.*, 2017, **19**, 1969–1982.

39 M. S. Holm, S. Saravanamurugan and E. Taarning, Conversion of sugars to lactic acid derivatives using heterogeneous zeotype catalysts, *Science*, 2010, **328**, 602–605.

40 W. Dong, Z. Shen, B. Peng, M. Gu, X. Zhou, B. Xiang and Y. Zhang, Selective Chemical Conversion of Sugars in

Aqueous Solutions without Alkali to Lactic Acid Over a Zn–Sn-Beta Lewis Acid–Base Catalyst, *Sci. Rep.*, 2016, **6**, 26713.

41 C. Hammond, D. Padovan, A. Al-Nayili, P. Wells, E. K. Gibson and N. Dimitratos, Identification of Active and Spectator Sn Sites in Sn-β Following Solid-State Stannation, and Consequences for Lewis Acid Catalysis, *ChemCatChem*, 2015, **7**, 3322–3331.

42 J. C. Jansen, E. J. Creyghton, S. L. Njo, H. van Koningsveld and H. van Bekkum, On the remarkable behaviour of zeolite beta in acid catalysis, *Catal. Today*, 1997, **38**, 205–212.

43 M. Moliner, Y. Román-Leshkov and M. E. Davis, Tin-containing zeolites are highly active catalysts for the isomerization of glucose in water, *Proc. Natl. Acad. Sci. U. S. A.*, 2010, **107**, 6164–6168.

44 E. Taarning, S. Saravanamurugan, M. Spangsberg Holm, J. Xiong, R. M. West and C. H. Christensen, Zeolite-Catalyzed Isomerization of Triose Sugars, *ChemSusChem*, 2009, **2**, 625–627.

45 C. Hammond, S. Conrad and I. Hermans, Simple and Scalable Preparation of Highly Active Lewis Acidic Sn-β, *Angew. Chem., Int. Ed.*, 2012, **51**, 11736–11739.

46 S. Shwan, J. Jansson, L. Olsson and M. Skoglundh, Effect of post-synthesis hydrogen-treatment on the nature of iron species in Fe-BEA as NH$_3$-SCR catalyst, *Catal. Sci. Technol.*, 2014, **4**, 2932–2937.

47 N. A. S. Ramli and N. A. S. Amin, Fe/HY zeolite as an effective catalyst for levulinic acid production from glucose: characterization and catalytic performance, *Appl. Catal., B*, 2015, **163**, 487–498.

48 M. P. Pachamuthu, K. Shanthi, R. Luque and A. Ramanathan, SnTUD-1: a solid acid catalyst for three component coupling reactions at room temperature, *Green Chem.*, 2013, **15**, 2158.

49 H. Y. Luo, L. Bui, W. R. Gunther, E. Min and Y. Román-Leshkov, Synthesis and Catalytic Activity of Sn-MFI Nanosheets for the Baeyer–Villiger Oxidation of Cyclic Ketones, *ACS Catal.*, 2012, **2**, 2695–2699.

50 B. Tang, W. Dai, G. Wu, N. Guan, L. Li and M. Hunger, Improved Postsynthesis Strategy to Sn-Beta Zeolites as Lewis Acid Catalysts for the Ring-Opening Hydration of Epoxides, *ACS Catal.*, 2014, **4**, 2801–2810.

51 Y. Román-Leshkov, M. Moliner, J. A. Labinger and M. E. Davis, Mechanism of glucose isomerization using a solid Lewis acid catalyst in water, *Angew. Chem., Int. Ed.*, 2010, **49**, 8954–8957.

52 M. Orazov and M. E. Davis, Tandem catalysis for the production of alkyl lactates from ketohexoses at moderate temperatures, *Proc. Natl. Acad. Sci. U. S. A.*, 2015, **112**, 11777–11782.